www.czasopisma.pan.pl PAN POLSKA AKADEMIA NAUK www.journals.pan.pl

Arch. Metall. Mater. **64** (2019), 2, 475-479

DOI: 10.24425/amm.2019.127562

HANEUL JANG*, KWANGMIN CHOI**#, JAEHYUCK SHIN**, DONGHYUN BAE**, HYUNJOO CHOI*

THE INFLUENCE OF GRAIN SIZE ON THE MECHANICAL DAMPING BEHAVIOR OF ALUMINUM

An understanding of the fundamental correlation between grain size and material damping is crucial for the successful development of structural components offering high strength and good mechanical energy absorption. With this regard, we fabricated aluminum sheets with grain sizes ranging from tens of microns down to 60 nm and investigated their tensile properties and mechanical damping behavior. An obvious transition of the damping mechanism was observed at nanoscale grain sizes, and the underlying causes by grain boundaries were interpreted.

Keywords: Al, Tensile properties, Damping behavior, Grain size

1. Introduction

The relative abundance and high specific strength of aluminum has contributed to its prominence as a structural material for use in the aerospace [1] and automotive [2] industries. In both of these industries, mechanical vibration tends to cause severe damage to the system, necessitating materials with good damping capacity as well as high strength/stiffness.

Many aluminum alloys, such as those of the 2000 (Al-Cu) [3], 6000 (Al-Mg-Si) [4] and 7000 series (Al-Zn-Mg-Cu) [5], have been reported to exhibit good mechanical damping by virtue of the interaction between dislocations and precipitates. However, materials exhibiting a high damping capacity usually also have a low yield stress and fatigue limit [6]. Although attempts have been made to enhance the strength of the matrix by introducing hard particles (e.g., Al2O3 [7], SiC [8], BaTiO3 [9], TiB2 [10] etc.), the damping capacity of composites below 400 K is not increased as compared to the Al matrix [9]. In order to achieve an optimal combination of high damping and good mechanical properties, manipulation of the crystalline structure has recently been attempted [12,13]. In this approach, a reduction of the quasicrystal grain size of Al-Cu-Fe to nanoscopic dimensions was reported to significantly increase its damping capacity, owing to the dissipation of mechanical energy in the nanostructured quasicrystals [11]. In addition, grain refinement of A356 alloy has also resulted in a simultaneous improvement in the damping capacity and mechanical properties [12,13].

A great deal of research has been focused on the effect of grain size on plastic deformation; and yet, its effect on mechanical damping is not well understood. In the present study, the strengthening behavior and damping capacity of coarse-, ultrafine- and nano-grained aluminum samples are compared, so as to investigate the role of grain boundaries in viscoelastic and plastic deformation.

2. Experimental

Three aluminum sheets, each with a different grain size, were produced by hot rolling ball-milled or pristine aluminum powders. High-energy ball milling of the aluminum powder (~150 μm diameter, 99.5 % in purity) was conducted using an attrition mill, in which a chamber was charged with aluminum powder (100 g) and stainless steel balls (~5 mm in diameter, 1500 g) to a ball-to-powder weight ratio of 15:1. This mixture was then stirred by horizontal impellers attached to a vertical shaft rotating at 550 rpm under a purified argon atmosphere at room temperature. Prior to milling, a control agent of 1 wt.% stearic acid (CH3(CH2)16CO2H) was added to prevent agglomeration and excessive cold welding of the powder during milling, and the outer surface of the chamber was cooled by circulating water. By varying the milling time (i.e., 0, 6, and 24 h), three separate aluminum powders were produced. These were then packaged in copper tubes with enveloped ends and compacted under ~200 MPa of pressure at room-temperature. Hot-rolling of the resulting material to a 12% reduction was conducted at 480°C, the thickness of the samples being ultimately reduced from 25 to 1.2 mm. Once the desired thickness was achieved, the copper tube was mechanically removed.

To estimate the grain size of the hot-rolled samples, X-ray diffraction (XRD, Rigaku, CN2301) with a Cu Kα radiation

* KOOKMIN UNIVERSITY, DEPARTMENT OF MATERIALS SCIENCE AND ENGINEERING, JEONGNEUNG-RO 77, SEONGBUK-GU, SEOUL, 02707, KOREA
** YONSEI UNIVERSITY, DEPARTMENT OF MATERIALS SCIENCE AND ENGINEERING, SEOUL, 03722, KOREA
# Corresponding author: hyunjoo@kookmin.ac.kr

source was utilized. Dog-bone type specimens (gauge length: 7 mm) were prepared from the hot-rolled aluminum sheets for the quasi-static uniaxial tension tests, which were aimed at investigating the mechanical properties of the hot-rolled sheets at room temperature. For these tests, an Instron-type machine with a constant crosshead speed and an initial strain rate of 1×10^{-4} s^{-1} was used. The mechanical damping capacities of the samples were evaluated by a dynamic mechanical thermal analyzer (DMTA) operating in a tensile oscillating mode, using rectangular plate samples measuring 20 mm×6 mm×1 mm that were obtained by machining and polishing. To examine the effects of temperature (T) and vibration frequency (f) on the damping capacity of each sample, tests were conducted at temperatures ranging from room temperature to 300°C, with a 3°C/min heating rate, at vibration frequencies of 0.5, 10, and 50 Hz.

3. Results and discussion

The X-ray diffraction patterns of the hot-rolled specimens are shown in Fig. 1(a), in which a peak broadening can be observed to have occurred as a result of the grain refinement during ball-milling. The mean grain size of the specimen milled for 24 h can be calculated from the Scherrer formula [14] $\beta_g(2\theta) = 0.9\lambda/d\cos(\theta)$, where $\beta_g(2\theta)$ is the breadth of the peak at half its maximum intensity, λ is the wavelength of the X-ray radiation used, θ is the Bragg angle, and d is the average grain size. For those specimens with a grain size greater than 100 nm, the grain size was determined from transmission electron microscope observations, as described in a previous report [15]. Figure 1(b) shows the mean grain sizes of the specimens as a function of their milling time. This shows that the grain size rapidly decreases with increasing milling time up to 6 h (~150 nm), then progressively saturates with increased milling, being reduced to ~56 nm after 24 h of milling. The samples produced from un-milled, 6-h-milled and 24-h-milled powders are hereafter denoted, respectively, as "coarse-grained" (CG), "ultrafine-grained" (UFG), and "nano-grained" (NG) on the basis of their observed grain sizes.

Curves of the tensile true stress (σ) versus true strain (ε) for each of the samples are plotted in Fig. 2(a), revealing a significant increase in the flow stress as the grain size is reduced.

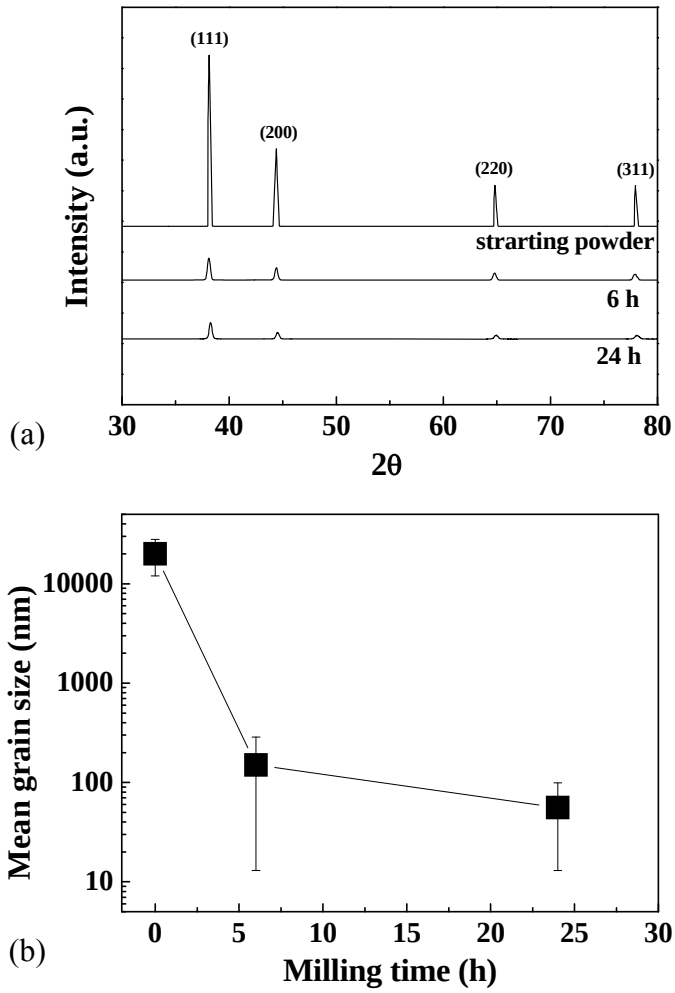

Fig. 1. (a) X-ray diffraction patterns of hot-rolled specimens and (b) mean grain size as a function of milling time

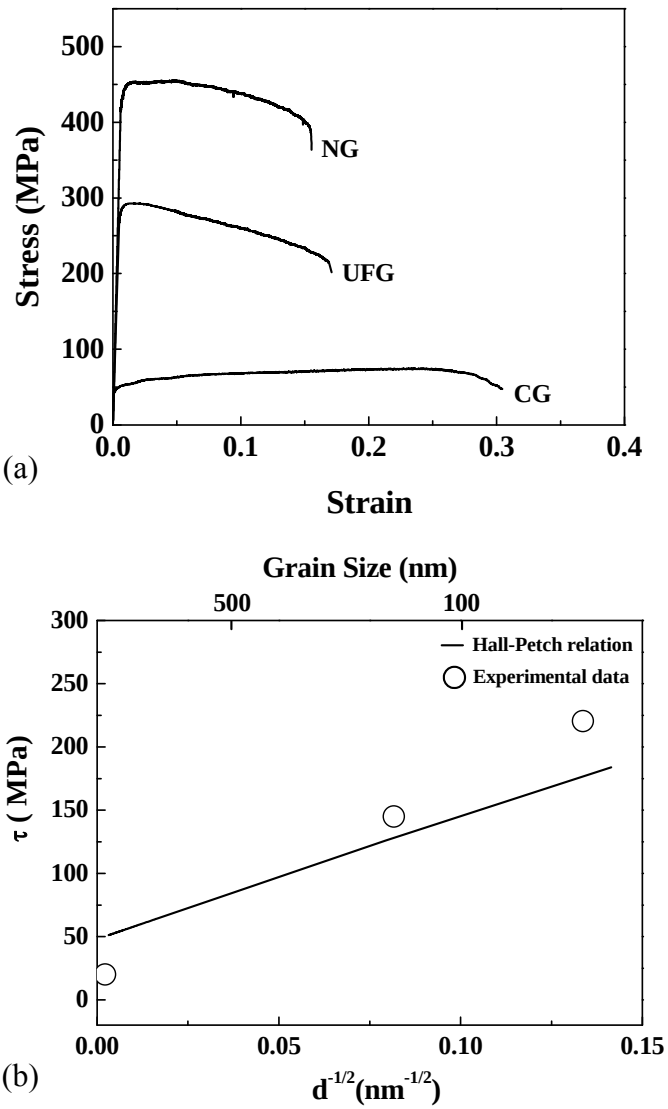

Fig. 2. Fig. 2. (a) Tensile true stress (σ) versus true strain (ε) curves, and (b) shear stress (τ) as a function of grain size ($d^{-1/2}$), together with the Hall-Petch relationship

Furthermore, the NG sample exhibits a yield strength that is 11 times greater than that of the CG sample; the NG aluminum also exhibits a strain softening under tension due to the plastic instability developed just after yielding. This effect has been demonstrated to be a result of shear localization in several nanocrystalline metals [16], the formation of shear bands being suggested as the dominant feature in the deformation of nanocrystalline metals and a direct consequence of the limited work hardening [17]. Consequently, while the CG aluminum sample shows a large elongation to failure at around 30 %, the NG aluminum exhibits quite low ductility (~15 %). Owing to this limited work hardening capacity of NG aluminum, it is prone to having an early onset plastic instability, thus leading to failure at a lower plastic elongation.

In Fig. 2(b), the yield stress obtained from the tensile test of each specimen is plotted as a function of the grain size ($d^{-1/2}$), together with the Hall-Petch relationship that is given as [18]:

$$\sigma_y = \sigma_0 + Kd^{-\frac{1}{2}} \tag{1}$$

where K is a constant and σ_0 is the intrinsic stress resisting dislocation motion in the deforming grains, here 0.2 kg mm$^{-2/3}$ and 9.8 MPa, respectively. From this, it can be seen that the yield stress follows the Hall-Petch strengthening behavior quite well down to a grain size of about 70 nm, which is indicative of lattice dislocation interactions with grain boundaries.

Interestingly, a positive deviation from the Hall-Petch relation is observed when the grain size is less than 70 nm. As the grain size is reduced below the dislocation mean free length, forest dislocations are unlikely to be accumulated within the grain, thus providing a transition in the deformation mechanism. Within this transition regime, various deformation mechanisms compete, with a predominance of twin or grain boundary sliding leading to a negative deviation from the Hall-Petch slope. For a variety of face-centered cubic (FCC metals) such as aluminum, copper, and nickel, deformation behavior has been believed to be additionally controlled in the form of atomic shuffling at the grain boundaries, leading to grain rotation or grain boundary sliding in small grains (<20 nm) [16,17,19]. When grain size is comparable to grain boundary width, stress required for grain boundary sliding is negligible because of reduced roughness of slide planes. A portion of grain boundary sliding contributing to total deformation will increase as grain size is reduced, providing a decrease in yield stress as the grain size decreases.

In contrast, this grain boundary sliding is insignificant at relatively large grain sizes of 50-70 nm. Furthermore, the partial dislocations and twins occasionally observed in other face-centered cubic (FCC) metals are not dominant due to the low twin ability and high stacking fault energy of aluminum [19]. Consequently, deformation tends to occur only via the activities of perfect dislocations, thereby leading to a positive deviation from the Hall-Petch relation.

The damping capacity (equivalent to internal friction) is the ability of a material to dissipate its energy during mechanical vibration under cyclic loading. Hence, the balance of energy loss (E'', loss modulus) and storage (E', storage modulus) can be quantified in terms of a loss tangent (tanΦ), as follows;

$$\bar{E} = \frac{\sigma}{\varepsilon} = \frac{\sigma_0}{\varepsilon_0}\left(\cos\Phi + i\,\sin\Phi\right) = E' + iE'' \tag{2}$$

$$\tan\Phi = \frac{E''}{E'} \tag{3}$$

where Φ is the loss angle by which the strain lags behind the stress [20]. For a perfectly elastic material, Φ is equal to 0 and σ/ε represents the elastic modulus, thus obeying Hooke's law. Since most materials are anelastic, the loss to storage modulus ratio has to be taken into account. When Φ is equal to 90, the material is considered to be perfectly viscous, as all mechanical energy would be dampened.

Damping of crystalline materials can be explained by several mechanisms, including: thermoelastic damping, magnetic damping, viscous damping, and defect damping [21-24]. The first three of these mechanisms originate as a consequence of the bulk response of a material. Defect damping, however, is an intrinsic factor, and early studies have revealed that it dominates the overall damping of a crystalline material [25-27]. This intrinsic damping can be mainly attributed to imperfections in the ordered structure, which include point defects (vacancies or self-interstitials) [25], line defects (dislocations) [26] and surface defects (grain boundaries) [27]. Among these, the effect of point defects is considered to be negligible within the temperature range of this study (below 300°C), whereas line defects or surface defects are thought to dominate mechanical damping. This means that the dislocations and grain boundaries are the main contributors to the overall damping.

Figure 3(a-c) shows tanΦ as a function of temperature for the CG, UFG, and NG aluminum samples at a test frequency of 0.5, 10, and 50 Hz, respectively. The damping capacity of the samples generally increases with temperature at all frequencies because the higher atomic vibration more effectively dissipates mechanical energy. In the low temperature region, the samples with the larger grain sizes have a higher damping capacity than NG aluminum. Interestingly, however, the damping capacity exhibits a transition temperature, after which the NG aluminum shows a much higher damping capacity than the UFG and CG aluminum. This transition temperature, at which the tanΦ value of NG aluminum begins to exceed that of UFG aluminum, is plotted as a function of the test frequency in Fig. 3(d), demonstrating that it increases with frequency.

High density of defects of NG aluminum can be considered as a cause of this transition temperature. As previously reported [28], severe grain refinement of materials can induce misoriented grains through repetitive straining, and this leads to grain boundaries with excessive extrinsic dislocations and exhibiting high-energy non-equilibrium configurations. In these regions of

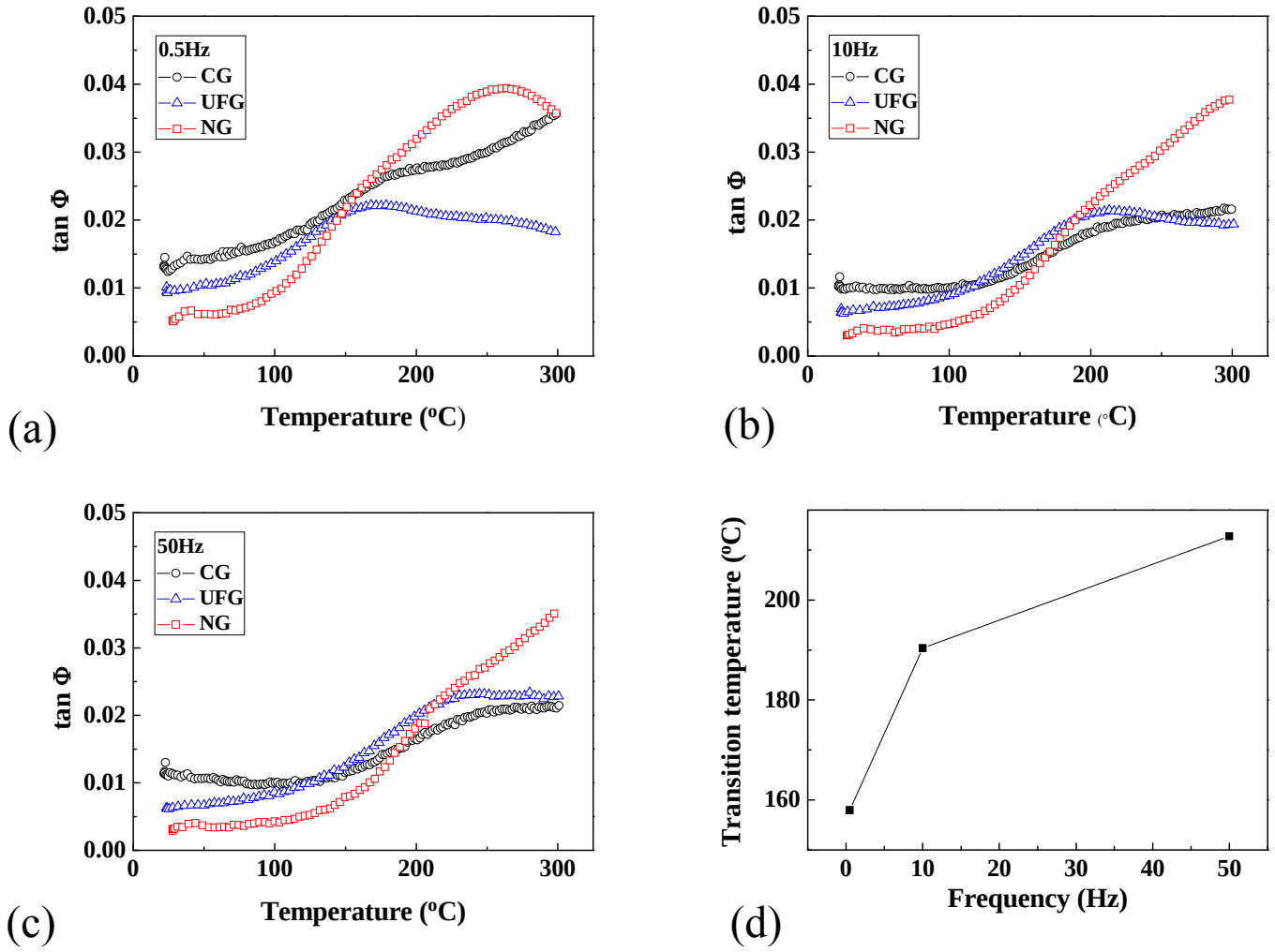

Fig. 3. (a-c) tanΦ as a function of temperature for CG, UFG, and NG aluminum at test frequencies of 0.5, 10, and 50 Hz, respectively, and (d) the transition temperature as a function of frequency

high imperfection density, an externally applied stress may be capable of causing atomic rearrangement and grain boundary sliding. If this is indeed the case, then atoms in non-equilibrium positions would be able to slide by one another, thus resulting in a viscoelastic-like behavior.

At lower frequencies, dislocations tend to be located at their low-energy configuration. Furthermore, a weak external stress cannot compete with the internal stress created by dislocation pile-ups. At high frequencies and high temperatures, however, the extrinsic grain boundary dislocations can be scattered quite effectively by mechanical vibration, thus contributing to mechanical damping. Consequently, the damping capacity of NG aluminum is superior to that of UFG or CG aluminum at high temperatures and high frequencies [29]. Moreover, the fact that the transition temperature shifts to a higher temperature with increasing frequency further confirms that boundary sliding becomes the main viscoelastic mechanism. Furthermore, UFG and NG specimens exhibit a typical internal friction peak while that NG aluminum is detected at higher temperatures compared to UFG aluminum. This also implies that the grain boundary sliding is likely to be responsible for a large portion of damping in NG aluminum [30].

4. Conclusions

The effect of grain size on the tensile and mechanical damping behavior of aluminum was investigated for grain sizes ranging from several micrometers down to ~50 nm. It was found that when the grain size was reduced below 70 nm, the metal loses its capacity for plastic deformation via dislocation slip, instead exhibiting positive yield stress deviations congruent with Hall-Petch behavior. The damping capacity of this nano-grained aluminum was also shown to be inferior to that of coarse-grained samples at low frequency and temperature, but also far exceeded them once a critical combination of temperature and frequency was applied. This is attributed to the fact that extrinsic grain boundary dislocations can scatter mechanical vibration quite effectively, and thus grain boundary activity can facilitate mechanical damping.

Acknowledgments

This work was supported by the National Research Foundation of Korea (NRF) Grant funded by the Korean Government (No.

Grant Number-2015R1A5A7037615, 2016M2B2A9A02943809 and 2017M1A3A3A02015639).

REFERENCES

[1] J.-P. Immarigeon, R.T. Holt, A.K. Koul, L. Zhao, W. Wallace, J.C. Beddoes, Mater. Charact. **35**, 41-67 (1995).
[2] M. Schimek, A. Springer, S. Kaierle, D. Kracht, V. Wesling, Phys. Procedia **39**, 43-50 (2012).
[3] C.Y. Xie, R. Schaller, C. Jaquerod, Mater. Sci. Eng. A **252**, 78-84 (1998).
[4] L. Liao, X. Zhang, H. Wang, Mater. Lett. **59**, 2702-2705 (2005).
[5] G.-C. Li, Y. Ma, X.-L. He, W. Li, P.-Y. Li, Trans. Nonferrous Met. Soc. China **22**, 1112-1117 (2012).
[6] Y.K. Favstov, Y.N. Shul'ga, A.G. Rakhshtadt, Metallurgia, Moscow, 272 (1980) (in Russian).
[7] R. Casati, M. Vedani, A. Tuissi, E. Villa, D. Dellasega, X. Wei, K. Xia, Microstructure and Damping Properties of Ultra Fine Grained Al Wires Reinforced by Al2O3 Nanoparticles, in: J. Grandfield (*Ed.*), Light Metals 2014, Springer International Publishing (2016).
[8] S. Salamone, B. Givens, K. Kremer, M. Aghajanian, Effect of Particle Loading on Properties, Damping, and Wear of AL/SiC MMCs, in: D. Singh (Ed.), Mechanical Properties Performance of Engineering Ceramics and Composites X, The American Ceramic Society (2015).
[9] G.-L. Fan, Z.-Q. Li, D. Zhang, Trans. Nonferrous Met. Soc. China **22**, 2512-2516 (2012).
[10] Y. Zhang, N. Ma, H. Wang, Y. Le, S. Li, Scripta Mater. **53**, 1171-1174 (2005).
[11] A.I. Ustinov, S.S. Polishchuk, V.S. Skorodzievskii, V.V. Bliznuk, Surf. Coat. Technol. **202**, 5812-5816 (2008).
[12] Y. Zhang, N. Ma, H. Wang, X. Li, Mater. Des. **29**, 706-708 (2008).
[13] A. Granato, K. Lücke, J. Appl. Phys. **27**, 583-593 (1956).
[14] H.P. Klug, L.E. Alexander, X-ray diffraction procedures, New York 1954.
[15] H.J. Choi, J.H. Shin, D.H. Bae, Compos. Sci. Technol. **71**, 1699-1705 (2011).
[16] Q. Wei, D. Jia, K.T. Ramesh, E. Ma, Appl. Phys. Lett. **81**, 1240-1242 (2002).
[17] M.A. Meyers, A. Mishra, D.J. Benson, Prog. Mater. Sci. **51**, 427-556 (2006).
[18] T.N. Baker, N.J. Petch, Yield, flow and fracture of polycrystals, London 1983.
[19] H.J. Choi, S.W. Lee, J.S. Park, D.H. Bae, Mater. Trans. **50**, 640-643 (2009).
[20] J. Zhang, R.J. Perez, C.R. Wong, E.J. Lavernia, Mater. Sci. Eng. R-Rep. **13**, 325-389 (1994).
[21] P. Lu, H.P. Lee, C. Lu, H.B. Chen, Int. J. Mech. Sci. **50**, 501-512 (2008).
[22] M. Oogane, T. Wakitani, S. Yakata, R. Yilgin, Y. Ando, A. Sakuma, T. Miyazaki, Jpn. J. Appl. Phys., Part 1 **45**, 3889-3891 (2006).
[23] S. Adhikari, J. Woodhouse, J. Sound Vib. **243**, 43-61 (2001).
[24] J. Zhang, R.J. Perez, E.J. Lavernia, J. Mater. Sci. **28**, 2395-2404 (1993).
[25] S. Kustov, S. Golyandin, K. Sapozhnikov, J. Pons, E. Cesari, J.V. Humbeeck, Acta Mater. **54**, 2075-2085 (2006).
[26] W. Johnson, J. Alloys Compd. **310**, 423-426 (2000).
[27] T. S. Kê, Phys. Rev. **72**, 41-46 (1947).
[28] Y. Koizumi, M. Ueyama, N. Tsuji, Y. Minamino, K. Ota, J. Alloys Compd. **355**, 47-51 (2003).
[29] R.R. Mulyukov, A.I. Pshenichnyuk, J. Alloy. Compd. **355**, 26-30 (2003).
[30] J. Gu, X. Zhang, M. Gu, M. Gu, X. Wang, J. Alloy. Compd. **372**, 304-308 (2004).